

Evolution and instabilities of disks harboring super massive black holes

Anna Curir ¹, Valentina de Romeri ¹, Giuseppe Murante ¹

© Springer-Verlag ●●●

Abstract The bar formation is still an open problem in modern astrophysics. In this paper we present numerical simulation performed with the aim of analyzing the growth of the bar instability inside stellar-gaseous disks, where the star formation is triggered, and a central black hole is present. The aim of this paper is to point out the impact of such a central massive black hole on the growth of the bar. We use N-body-SPH simulations of the same isolated disk-to-halo mass systems harboring black holes with different initial masses and different energy feedback on the surrounding gas. We compare the results of these simulations with the one of the same disk without black hole in its center. We make the same comparison (disk with and without black hole) for a stellar disk in a fully cosmological scenario. A stellar bar, lasting 10 Gyrs, is present in all our simulations.

The central black hole mass has in general a mild effect on the ellipticity of the bar but it is never able to destroy it. The black holes grow in different way according their initial mass and their feedback efficiency, the final values of the velocity dispersions and of the black hole masses are near to the phenomenological constraints.

Keywords galaxies: spirals, structure, evolution, halos, black holes

1 Introduction

In a series of recent papers Curir et al. (2006), Curir et al. (2007), Curir et al. (2008) we have shown that the bar formation inside disk galaxies is triggered also by the cosmological scenario and not only by the classical instability of a self gravitating disk. We obtained such

result by analyzing the growth of a bar instability in exponential disks, embedded in a Dark Matter (DM) halo which evolves in a cosmological context. We used purely stellar disks as well as disks containing both gas and stars. In the latter case, we studied the effect of only allowing the gas to radiatively cool, and we then examined the impact of the star formation. Our embedding technique allowed us to vary the baryon to DM mass ratio onto the *same* DM halo. In almost all the cases we studied, including the classically stable ones, we noticed the formation of a long-lasting bar. The onset of the bar instability, in the latter cases, appears to be driven by the triaxiality and by the dynamical evolution of the DM halo. For a few cases, cooling gas proved to be able to stabilize the gas, but such effect disappeared when star formation was turned on, because gas converts in stars before a stabilizing, dense, central knot can form. Therefore the problem of inhibiting the bar formation is still an open astrophysical problem, since one third at least of disk galaxies are not barred.

The observational data indicate that massive central black holes exist in disk galaxies as well as ellipticals. Moreover black holes masses are correlated with host galaxies properties; Magorrian et al. (1998) has concluded that the median black holes mass is 0.006 of the bulge mass and Kormendy & Gebhardt (2001) correlated the black hole mass to the bulge velocity dispersion. Such a large mass concentration inside the galaxy could affect its structure. It is known indeed that a central mass concentrations (CMC) can destroy a bar (see e. g. Bournaud et al. (2005), Curir et al. (2007)). The effect of the presence of a massive black hole (BH) at the center of a disk galaxy could therefore mimic the stabilizing action of a knot of dense, cold gas which forms if gas is allowed to radiatively cool but not to form stars.

The influence of central BHs on the dynamical evolution of bars in disk galaxies has been examined mainly

Anna Curir , Valentina de Romeri , Giuseppe Murante

¹INAF-Osservatorio Astronomico di Torino. Strada Osservatorio 20 -10025 Pino Torinese (Torino). Italy. e-mail:curir@oato.inaf.it

by Shen & Sellwood (2004) and Hozumi & Hernquist (2005) in a pure non dissipative scenario and using as model galaxies isolated systems. Their results give very high values ($10^{8.5}$) the minimum mass necessary for bar dissolution, higher than the inferred one for local spirals.

In this paper we want to treat the same problem using simulations of stellar- gaseous disk with star formation. We will evolve the disk model as isolated system and in a cosmological scenario. We will discuss the evolution of the bar ellipticity and semi-major axis of the same disk endowed with different initial BH mass. The BH is accreting during the evolution. Its accretion is regulated by a suitable feedback parameter (Di Matteo et al. (2003)), which states a coupling between a percentage of the accretion radiating energy and the gas heating. We will also show the role of this feedback parameter and its interplay with the initial BH mass, the formation of the CMC and with the star formation.

Finally, we will investigate the relation between the decrease of the bar ellipticity, the accretion time and the feedback. Moreover we will compare our simulations with some phenomenological issues as the Kormendy black hole mass-bulge velocity dispersion relation.

The plan of the paper is the following. In Section 2, we summarize our recipe for the initial *disk + halo* system and present the star formation recipe. In Section 3, we present our simulations, and in Section 4 we point out our results. The parameters related to the bars formed in the new and the old stars and to the global, old+new, stellar populations are given in this section. In section 5 there are phenomenological implications and section 6 is devoted to our discussion and conclusions.

2 Method

In the cosmological simulations, we embed a gaseous and stellar disk inside a cosmological halo selected in a suitable way, as to be able to host a disk galaxy, and follow its evolution inside a cosmological framework: a Λ CDM model with $\Omega_m = 0.3$, $\Omega_\Lambda = 0.7$, $\sigma_8 = 0.9$, $h = 0.7$, where Ω_m is the total matter of the Universe, Ω_Λ the cosmological constant, σ_8 the normalization of the power spectrum, and h the value of the Hubble constant in units of $100h^{-1} \text{ km s}^{-1} \text{ Mpc}^{-1}$. The halo is extracted from the cosmological simulation at a given redshift (we chose $z = 2$). The stellar+gaseous disk is embedded in the halo, in equilibrium with its gravitational potential as in the isolated case; the system is then re-inserted in the full cosmological simulation

and evolved. A detailed description of our method of producing the cosmological scenario where the disk is evolved was given in Curir et al. (2006).

As far as the isolated simulations is concerned, we embed a gaseous and stellar disk inside a DM halo, having a radial density profile of the NFW form Navarro et al. (1996) and follow its evolution for 10 Gyrs. The halo has a mass of $1.36 \times 10^{11} h^{-1} M_\odot$ and initial concentration $c=4.5$. The disk is set in equilibrium with the gravitational potential of the DM halo, but not *vice-versa*; as a consequence, there is a transient period in which the halo responds to the disk immersion. In Curir (2006) we showed that our embedding procedure is not triggering, *per-se*, a bar instability, and as well, no instability is triggered because of our chosen numerical resolution.

The units of our simulations are: $10^{10} h^{-1} M_\odot$ for the mass, $1 h^{-1} \text{ kpc}$ for the length, $0.98 h^{-1} \text{ Gyrs}$ for the time.

2.1 The baryonic disk

The spatial distribution of particles follows the exponential surface density law: $\rho = \rho_0 \exp(-(r/r_0))$ where r_0 is the disk scale length, $r_0 = 4h^{-1} \text{ Kpc}$, and ρ_0 the surface central density. The disk is truncated at five scale lengths with a radius: $R_{disk} = 20h^{-1} \text{ Kpc}$. Its mass is $1.9 \times 10^{10} h^{-1} M_\odot$.

This value of mass has been chosen and employed in the previous papers as the critical one for the bar instability: the disk/halo mass ratio for this case is in the instability range from the classical point of view, the presence of a cold gas knot originated by gas cooling does stabilize it against the bar formation, and it becomes unstable again if the gas is allowed to form stars.

To obtain each disk particle's position according to the assumed density distribution, we used the rejection method Press et al. (1986). We used 56000 star particles and 56000 gaseous particles to describe our disk. The masses of gas, stellar and DM particles are respectively $7 \times 10^4 h^{-1} M_\odot$, $2.8 \times 10^5 h^{-1} M_\odot$, $1.194 \times 10^6 h^{-1} M_\odot$. The (Plummer equivalent) softening length, the same for DM, gas, and star particles and black hole, is $0.5h^{-1} \text{ kpc}$.

In the cosmological case we embed the disk in the high-resolution cosmological simulation, at redshift 2, in a plane perpendicular to the angular momentum vector of the halo and in gravitational equilibrium with the potential. Its center of mass corresponds to the position of the DM particle having the minimum value of gravitational potential. The initial redshift corresponds to 10.24 Gyrs down to $z = 0$ in our chosen cosmology.

During the evolution, new star particles are formed from the gaseous particles. We refer to such new component as ‘new star component’, whereas we will call ‘old star component’ the non dissipative particles present in the disks at $z = 2$ (at $t = 0$ in the isolated cases).

In the disk center of mass resides a BH which is represented as a collisionless, heavy mass point. It is able to swallow the gas in its neighborhood. The feedback parameter ϵ_f assigns a certain percentage of the accretion energy to be thermally coupled with the gaseous component. This feedback regulates the BH accretion, which, without such effect, is catastrophic. The default value of such parameter is $\epsilon_f = 0.05$ (see below), but we will explore in the paper other different values. We used the BH/energy feedback model of Di Matteo et al. (2003). This model hypothesizes that the gas accretion is limited by the Eddington rate:

$$\dot{M} = \frac{4\pi GM_{BH}m_p}{\epsilon_r\sigma_{TC}}$$

where M_{BH} is the BH mass, m_p the proton mass, σ_T the Thompson cross section and ϵ_r the radiative efficiency. We follow Di Matteo et al. (2003) and set $\epsilon_r = 0.1$. A fraction ϵ_f of the energy emitted by the BH couples with the surrounding gas, giving an energy output rate of $E_{feed} = \epsilon_f\epsilon_r M_{BH}c^2$. The parameter ϵ_f is the feedback parameter.

2.2 Star formation recipe

We use the sub-grid star formation prescription by Springel & Hernquist (2003). In it, when a gas particle overcomes a given density threshold its gas content, is considered to reside in a multi-phase state, that corresponds to the equilibrium solution of an analytical model describing the physics of the multi-phase interstellar medium. Such a solution gives an effective temperature for the gas particle, obtained as a weighted average of the (fixed) temperature of the cold phase and of the hot phase. The temperature of the hot phase is set by supernova feedback and by the efficiency of cloud evaporation. The resulting inter stellar medium (ISM) has an effective equation of state $P_{eff}(\rho)$, which is stiffer than isothermal and prevents Toomre instabilities even when a large amount of gas is present. When this prescription is used, the star formation rate agrees with the Schmidt law in disk galaxies, as obtained e.g. by Kennicutt (1998). The effective temperature drives hydrodynamical interactions of the gas particles. Moreover, the model consistently gives a star formation rate, which is used to spawn a star particle from the gas one on the basis of a stochastic prescription; the initial

mass function adopted is the Salpeter’s one. The star-forming from the gas has the same position and velocity as the gaseous particle.

3 Simulations

We performed 11 simulations of a disk+halo isolated system, and 2 Cosmological simulations, where the disk was embedded in our selected cosmological halo. We exploited the non-public version of the parallel Tree+SPH N-body code GADGET-2 (Springel 2005) (courtesy of V. Springel). The simulations run on the CLX computers located at the CINECA computing center (BO, Italy). The configurations have been evolved for 10.44 Gyrs (t_{fin}).

The main parameters and the final properties of our set of simulations are listed in Table 1. We kept fixed the disk mass and the gas to stellar mass ratio, and varied the initial BH mass and the feedback strength ϵ_f . We focused on the effect of the presence of a BH on the bar instability, and refer the reader to our previous works Curir et al. (2006), Curir et al. (2007), Curir et al. (2008) for a study of the impact of other significant parameters of our disk+halo system on such instability.

As a geometrical global measure of the bar strength, we defined the value of the ellipticity, $\epsilon = 1 - b/a$, (where a, b are the semi-axes of the contour) chosen on the iso-density level where such a value is maximum.

We defined the *bulge* as the total mass contained inside a radius centered on the new stars center of mass and corresponding to a minimum thickness of $4h^{-1}kpc$. The bulges in our simulations are ‘‘pseudobulges’’ as defined in Kormendy et al. (2002). The initial disk is bulgeless and the bulge is formed by secular instability and accreted by the formation of the new stars. In our simulations the timescale of the formation of these pseudobulges is 3-4 Gyrs. The final masses consisting of old and new stars are between $6 \times 10^9 h^{-1}M_\odot$ and $7 \times 10^9 h^{-1}M_\odot$.

In Table 1 we present the simulation number (I column), the initial mass of the BH in code units (II col.), the feedback value, i.e. the percentage of accretion energy coupled with the gas heating (III col.). Moreover, as final values we present the maximum ellipticity for the old star system(IV col.) and for the new star (V col.), the final mass of the accreted BH (VI col.), the major axis corresponding to the maximum ellipticity for the old stars (VII col.)and for the new stars (VIII col.), the central mass concentration CMC defined as the mass of all the components (stars, new stars and gas) inside a radius of $1.5h^{-1}kpc$ followed by the mass fraction of BH to the CMC (IX col.) and the time needed for the accreting BH to reach the value $10^8 h^{-1}M_\odot$.

Table 1 Simulations: o.s.=old stars , n.s.= new stars. Masses are in units of $10^{10}h^{-1}M_{\odot}$, lengths in h^{-1} kpc, times in Gyrs

N	BH m_{ini}	ϵ_f	ϵ (o.s.)	ϵ (n.s.)	BH m_{fin}	a_{max} (o.s.)	a_{max} (n.s.)	CMC - BH $_{frac}$	$t_{BH=10^8}$
i1	10^{-6}	0	0.747	0.75	0.18	6.37	1.6	0.23 - 0.72	6.289
i2	0.001	0	0.43	0.44	0.23	6.28	6.27	0.3 - 0.76	2.05
i3	0.005	10^{-4}	0.845	0.85	0.021	7.7	1.2	0.19 - 0.11	0.993
i4	10^{-5}	0.05	0.8	0.81	6.8×10^{-5}	7.94	1.5	$0.22 - 10^{-4}$	$t > t_{fin}$
i5	10^{-4}	0.05	0.69	0.71	1.15×10^{-4}	6.16	6.6	$0.14 - 8.2 \times 10^{-4}$	$t > t_{fin}$
i6	10^{-4}	0.01	0.74	0.82	$2. \times 10^{-4}$	3.45	1.31	$0.15 - 1.3 \times 10^{-3}$	$t > t_{fin}$
i7	0.001	10^{-5}	0.58	0.49	0.21	6.59	3.73	0.16 - 1.3	0.1667
i8	0.001	$5. \times 10^{-5}$	0.77	0.69	0.027	8.29	2.49	0.19 - 1.42	1.389
i9	0.001	10^{-4}	0.73	0.75	0.014	8.16	1.96	0.18 - 0.078	5.49
i10	0.001	0.001	0.83	0.83	0.0024	6.72	1.21	0.16 - 0.015	$t > t_{fin}$
i11	0.001	0.01	0.74	0.85	0.0018	7.8	1.36	0.17 - 0.01	$t > t_{fin}$
c1	0.001	$5. \times 10^{-5}$	0.53	0.477	0.0065	8.18	4.08	0.15 - 0.04	$t > t_{fin}$
c2	0	0	0.476	0.48	0	7.2	3.8	0.1	$t > t_{fin}$

4 Results

Our main result is that in all of our simulations, a stellar bar is still living at the final time in the old star component. The new star component at the end of our runs is arranged in a bulge component which presents a more or less barred shape depending on the initial mass of the BH and on the feedback. Overall, the presence of a BH is never able to quench the stellar bar, not even when its mass is significantly larger than allowed by observations.

An example of the final configuration is shown in Fig. 1 for simulation i8. Fig 1 has been constructed with the same box-size, number of levels, and density contrast as in Papers 1, 2 and 3.

In Fig. 2 we show the value of the ellipticity of the bar at the final time, as function of the final mass of the BH. Only results for simulations having the same initial masses of the BH ($10^7h^{-1}M_{\odot}$) are shown here. The final BH mass is a direct function of the feedback parameter, the larger one corresponding to a simulation with no BH feedback. This diagram show a clear, if obvious, correlation for the masses larger than $10^8h^{-1}M_{\odot}$: more massive black hole-weaker bar. In particular, the point of lower ellipticity in such figure correspond to the final time of simulation i2, where the feedback parameter is zero and the BH mass is $2.3 \times 10^9h^{-1}M_{\odot}$, a value higher than the minimum mass requested by Hozumi & Hernquist (2005) for a complete bar destruction. In our case the bar instability is not totally inhibited, but the ellipticity is the weakest one.

In Fig. 2 the peak in the ellipticity corresponding to a feedback $\epsilon_f = 0.001$ (simulation i10) is created by

the competition between two effects: the star formation which is working in favor of the bar (and which is weakened by the BH feedback) and the increase of the central BH mass + CMC, which is inhibiting the bar. The star formation rate increases moving from the first to the second point of diagram 2 (because the BH feedback decreases), it is stationary going to the third point (but the central BH mass + CMC has increased enough to weaken the ellipticity) and it decreases again after.

More details about the impact of the BH on the ellipticity are in Fig. 3, where we see the final ellipticity profile, as a function of the semi-major axes of the iso-density contours for the simulations of Fig. 2.

In Table 1, we see that the values of the CMC are different for different simulations and in most of the cases they are bigger, or much bigger than the BH final mass. Therefore one can deduce that the effect of the black hole in the disk center is not really a direct gravitational impact on the bar, but more an effect of modulating and, for the more massive BH and lower feedback values, enhancing the CMC formation, which, in turn, has an effect on the bar ellipticity. In Fig. 4 we have shown the direct correlation between the final BH mass and the CMC: the more the black hole is massive, the higher is the CMC. In Fig.4 we present only the cases starting with the same initial BH mass: as in Fig. 2, more massive BHs correspond to lower values of the feedback. In the same figure, we show an horizontal line: the value of the CMC for the case of the disk without BH. It is evident that for the higher values of the feedback (first three points of the diagram), the value of the CMC is reduced by the gas heating, when compared with the CMC of the same disk without a central BH. The difference in CMC between cases with

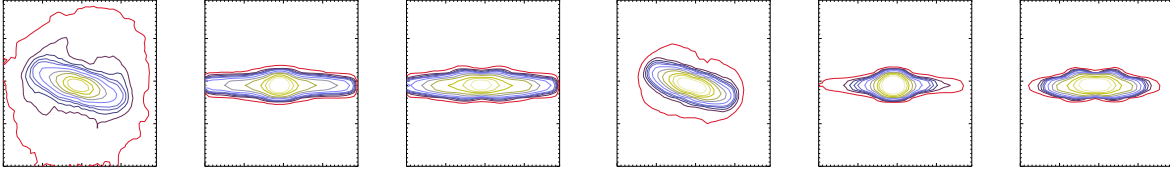


Fig. 1 iso-density contours of old stars in the planes xy , xz and yz (left three panels) and new stars (right panels) for simulation i8, at the end of the evolution

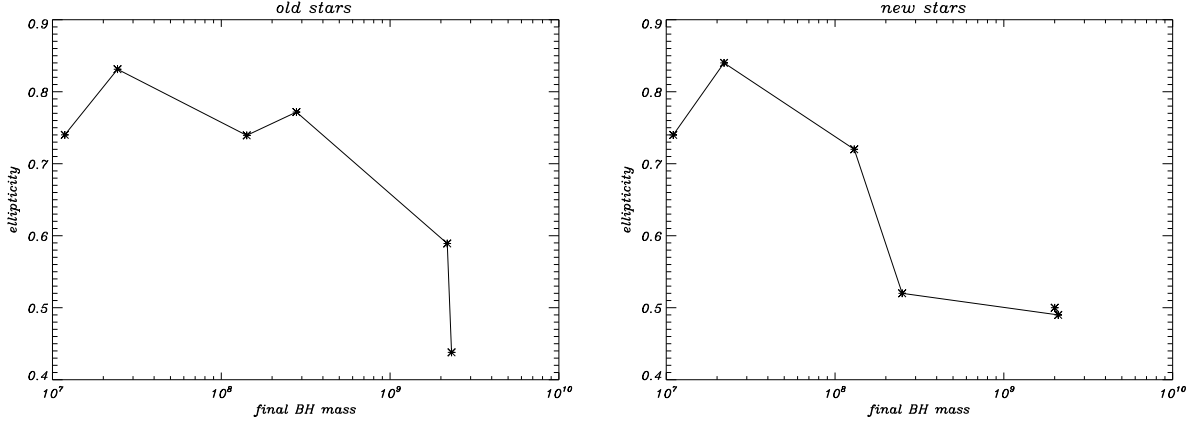


Fig. 2 Ellipticity as function of the final mass (in solar masses) of the BH for the simulations with the same BH's initial mass ($10^7 h^{-1} M_{\odot}$).

strong feedback and weak one is almost completely due to the new stars component and to the gas content.

We also compared the effect of having different evolutionary patterns of our central BH on the onset of the bar, i.e. different initial BH masses with different feedback efficiencies. With this aim, we looked for the time t at which the mass of the BH is equal to the value $10^8 h^{-1} M_{\odot}$, independently of the initial BH mass. We then plotted in Fig 5 the ellipticity as a function of the time t needed for the BH to reach such a mass value.

We can disentangle the effect of the bar evolution by comparing the bar ellipticities measured in the same disk, at the same times, in a simulation without a central BH (dotted line in Fig.5).

This comparison shows that a too fast or too slow growth of the BH results in a small effect on the bar ellipticity. A significant change of ellipticity, with respect to the simulation without the BH, only happens if the BH takes from 2 to 5 Gyrs to reach a mass of $10^8 M_{\odot}$. Of course, the subsequent evolution of the bar *does* depend on the mass of the BH; a BH which quickly reaches our reference mass and then continues to grow, will have a larger effect on the bar ellipticity at the final time, as shown in Figure 2.

In Fig.6 and 7 we provide the profiles of the *differences* of the ellipticities with and without the BH, for the old (Fig. 6) and the new (Fig.7) stars at the same

times as in Fig. 5., i.e. when the BH mass reaches the value $10^8 M_{\odot}$. These differences are always negatives, for the new stars except for $t=2.05$ (case i2 in Tab. 1), meaning that for all the other times, the bar is stronger at all radii if the BH is not present.

For the old stars profiles the trend is less evident: at some times we have radii in the disk where the ellipticities of the bar containing the BH is slightly higher. But it is evident that the differences are always negative at all times as far as the internal radii is concerned. We interpret this as the confirm that the effect of the BH is to decrease the strength of the inner bars. This is consistent with the findings of Holley-Bockelmann et al. (2002) which however only considered the stellar component in a triaxial system and used an adiabatically growing potential to simulate the presence and growth of the central BH. They noticed that the major impact of the BH on the triaxiality of the galaxy involves at maximum the 10% inner mass of the galaxy. We estimated indeed that the major impact on the variation of the ellipticity is on the *inner* iso-density contour, containing $\approx 10\%$ of the mass, when the BH is present with respect to our control case.

These results are qualitatively confirmed even if we evaluate the ellipticity using the inertial tensor inside our stellar system.

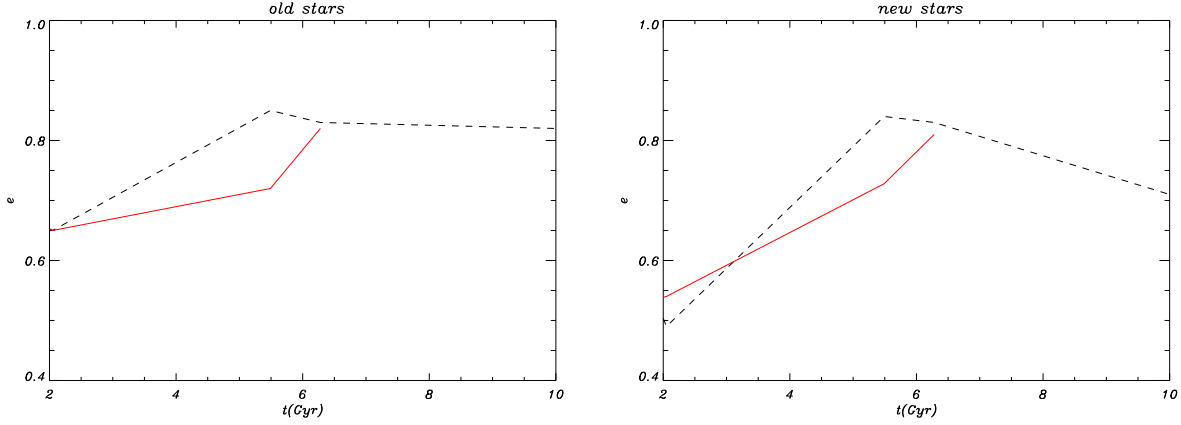


Fig. 5 Ellipticity of the bar when the accreting BH reaches the value $10^8 h^{-1} M_\odot$, as function of the time accretion (solid line). Ellipticity at the same time for a disk without central BH (dashed line). The ellipticity is evaluated for old star (left panel) and new stars (right panel)

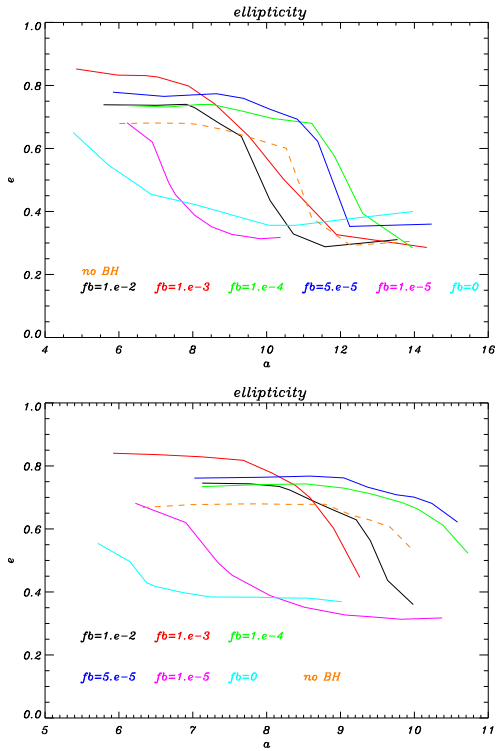


Fig. 3 Profiles of the ellipticity at the final time for the set of simulations with the same initial BH mass $10^7 h^{-1} M_\odot$ and different feedback. The profiles are for the old stars component (upper panel) and for the new one (lower panel)

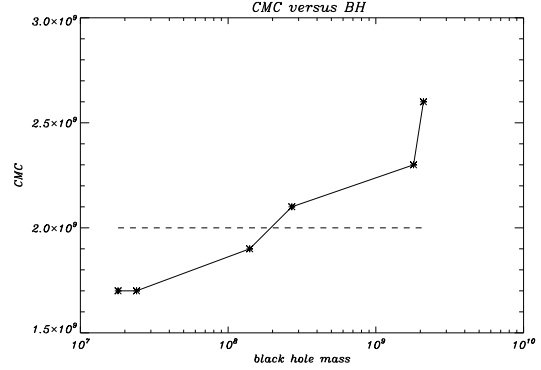


Fig. 4 Final central mass concentration (in solar masses) versus final BH mass (in solar masses), for the cases having the same initial BH mass. The horizontal line indicates the value of the final CMC in the case of the disk without BH.

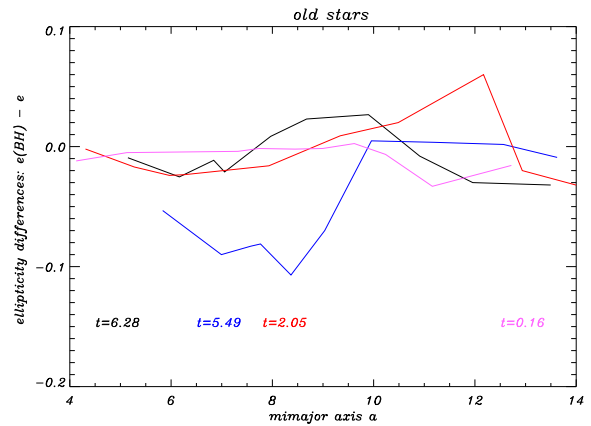


Fig. 6 Differences between ellipticity profiles of the stellar bar (old stars) with ($e(BH)$) and without (e) the BH, when the accreting BH reach the value $10^8 h^{-1} M_\odot$, the different colors correspond to different accretion times.

4.1 Cosmological cases

4.1.1 bar strength

We performed two cosmological simulations, one with a BH having a mass $M_{BH} = 10^7 h^{-1} M_{\odot}$ (c1) and another without the BH (c2). We chose $\epsilon_f = 5.10^{-5}$ as our feedback parameter. We used the embedding procedure described in Curir et al. (2006). The values of the ellipticities show a very mild impact of the BH on the onset of the bar instability and its evolution. In Table 1 we reported the final ($z = 0$) value of the bar ellipticity, which is very similar in the two cosmological cases both in the old and in the new stellar component. Note that, for the cosmological run, we used a quite high BH initial mass and a low feedback parameter. Such parameter choice is the one which shows to be the most effective in dumping the bar instability in our isolated cases (case i8 in Table 1). Even so, the presence of the central BH has practically no inhibiting effect on the bar instability.

4.1.2 DM concentration

In this section we investigate if the BH has an impact on the concentration parameter of the haloes. We then compare three different haloes: the halo from our original DM-only simulation, selected for the disk immersion; the same halo containing the disk, and the same halo containing the disk and the BH.

In the table 2 we show the behavior of the NFW concentration parameter as a function of the redshift z in the three cases. It is known that the baryonic matter has an influence on the halo concentration increasing it by an amount that Lin et al. (2006), e.g, estimated to be around 10%. Moreover, the concentration evolves approximately linearly with redshift (see

e.g. Bullock et al. (2001)); at redshift $z = 2$ we expect a concentration parameter of the order of one third that found at $z = 0$. Our DM halo shows a concentration evolution which is evolving more than linearly: it increases by a factor ≈ 4 from $z = 2$ to $z = 0$. In the Table, we also show the increase in the concentration of the DM halo due to the presence of the baryonic disk only (case c1). This increase is higher than the expected 10%. On the other hand, from the table it is clear that the presence of a BH has practically no effect on the concentration parameter.

5 Kormendy relation

Figure 8 shows the values of the stellar velocity dispersion inside the bulges at the end of the evolution as function of the BH masses.

We compared data from our simulations with observations by Kormendy et al. (2002). Data from our simulations are located in the pseudo-bulges region, with is consistent with the origin of the bulge structure in our simulations: they are not classical hot bulges, rather, they derive from secular evolution of the bar.

We can't find the phenomenologically observed correlation of velocity dispersions with the BH masses. It must be noticed that we vary the BH mass and feedback parameter within the *same* DM halo, so from this point of view our Fig. 8 simply suggest that varying the feedback efficiency and the initial BH mass has no effect on the stellar velocity dispersion, which remains a reasonable proxy for the halo mass.

The values that better agree with observation are obtained from simulations using a high BH feedback parameter. This trend suggests an useful constraint for such parameter in the simulations. Another possibility is that pseudo-bulges could behave differently, in this regard, from hot bulges. This point remains to be deepened both observationally and theoretically.

6 Discussion and conclusions

We have presented 11 isolated simulations and 2 cosmological simulations of the evolution of a stellar+gaseous disk embedded in a DM halo, with the same disk-to-halo mass ratios. The aim was to evaluate the impact of a massive black hole, with different accretion histories on the formation and evolution of a stellar bar.

The old star component shows a long-lasting bar, 10 Gyrs old, in all our simulations, regardless of the presence, the mass and the energy feedback efficiency of a central BH.

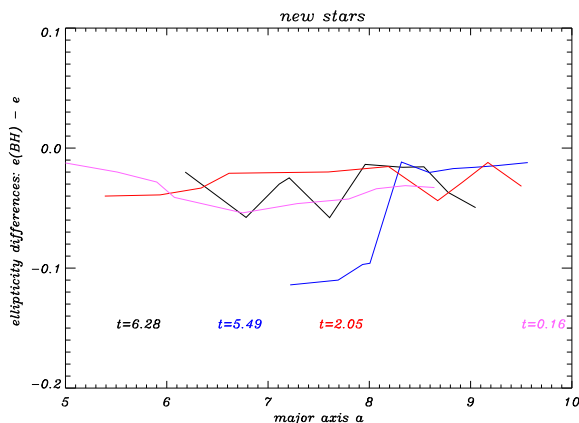


Fig. 7 Same as in the previous figure, but for the new stars.

Table 2 Halo concentrations

z	halo	c1	c2
2	4.5	4.5	4.5
1	8.8	12.8	12.9
0	19.7	29.1	29.9

We noticed a mild impact of the BHs having masses greater than $10^8 h^{-1} M_\odot$ on the old star component ellipticity, impact which appear stronger on the bar ellipticity of the new stars. In a previous paper (Curir et al. (2008)) we found that the star formation, by reducing the central gaseous mass concentration, allows the bar to survive until the end of the evolution in massive disks, at variance with the results in Curir et al. (2007) (where the gas was not allowed to form stars): in the latter case a gas fraction 0.2 was able to destroy the bar.

In this work we show that a BH placed and growing at the center of the disk has a small influence on the ellipticity of the bar developing in the preexistent star population. On the other hand, the BH with its feedback has an action on the formation of the CMC, which has a major role in quenching the bar. The bar formed by the newly formed stars is always weaker than in the disk without BH, independently on the BH’s evolution and feedback. Also in this case, however, the presence of the BH does not completely stop the bar formation.

A direct comparison between the results of our N -body simulations and the results of Hozumi & Hernquist (2005) is not possible. The reason is that their numerical model consists in a razor-thin disk model, without bulge and halo. It is evolved using a self-consistent field method (Hernquist & Ostriker (1992)), and not with a N -body code. Whereas the Hozumi’s disk is stabilized by a black hole having mass of $10^{8.5} M_\odot$ our disk forms a bar even if the central BH has a higher mass.

Adding gas and star formation to the same disk, we notice that an accreting massive BH has an impact on the bar ellipticity but it is not able to destroy it completely.

The effect of the BH is more evident on the *inner* bar ellipticity, which is reduced also when the effect of a star-forming gaseous component is considered.

A comparison with the phenomenology confirms that the default feedback parameter value 0.05 seems the more appropriate to reproduce the correlations between the velocity dispersion and the black holes masses observed by Kormendy.

Acknowledgments Simulations were performed on the CINECA IBM CLX cluster, thanks to the INAF-CINECA grants cnato43a/inato003 “ Simulations of disk galaxies in a cosmological framework: the impact of the central Black Hole”. We wish to thank

V. Springel for kindly providing us with his code GADGET. We thank an anonymous referee for his/her valuable suggestions, helpful to improve the paper.

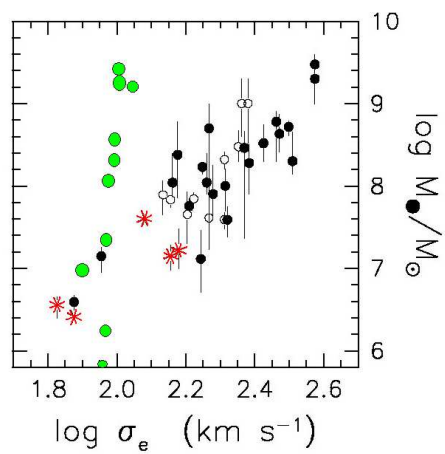


Fig. 8 The BH masses versus the velocity dispersions in our simulations (green points) compared with the Kormendy observed data (cit)

References

- Bournaud, F., Combes, F., & Semelin, B. 2005, *Mon. Not. R. Astron. Soc.*, 364, L18
- Bullock, J. S., Kolatt, T. S., Sigad, Y., et al. 2001, *Mon. Not. R. Astron. Soc.*, 321, 559
- Curir, A., Mazzei, P., & Murante, G. 2006, *Astron. Astrophys.*, 447, 453
- Curir, A., Mazzei, P., & Murante, G. 2007, *Astron. Astrophys.*, 467, 509
- Curir, A., Mazzei, P., & Murante, G. 2008, *Astron. Astrophys.*, 481, 651
- Di Matteo, T., Croft, R. A. C., Springel, V., & Hernquist, L. 2003, *Astrophys. J.*, 593, 56
- Hernquist, L. & Ostriker, J. P. 1992, *Astrophys. J.*, 386, 375
- Holley-Bockelmann, K., Mihos, J. C., Sigurdsson, S., Hernquist, L., & Norman, C. 2002, *Astrophys. J.*, 567, 817
- Hozumi, S. & Hernquist, L. 2005, *Publ. Astron. Soc. Jpn.*, 57, 719
- Kormendy, J., Bender, R., & Bower, G. 2002, in *Astronomical Society of the Pacific Conference Series*, Vol. 273, *The Dynamics, Structure History of Galaxies: A Workshop in Honour of Professor Ken Freeman*, ed. G. S. Da Costa & H. Jerjen, 29+
- Kormendy, J. & Gebhardt, K. 2001, in *American Institute of Physics Conference Series*, Vol. 586, *20th Texas Symposium on relativistic astrophysics*, ed. J. C. Wheeler & H. Martel, 363+
- Lin, W. P., Jing, Y. P., Mao, S., Gao, L., & McCarthy, I. G. 2006, *Astrophys. J.*, 651, 636
- Magorrian, J., Tremaine, S., Richstone, D., et al. 1998, *Astron. J.*, 115, 2285
- Navarro, J. F., Frenk, C. S., & White, S. D. M. 1996, *Astrophys. J.*, 462, 563
- Press, W. H., Flannery, B. P., & Teukolsky, S. A. 1986, *Numerical recipes. The art of scientific computing* (Cambridge: University Press, 1986)
- Shen, J. & Sellwood, J. A. 2004, *Astrophys. J.*, 604, 614
- Springel, V. 2005, *Mon. Not. R. Astron. Soc.*, 364, 1105